Journal of Fiber Bioengineering and Informatics 7:3 (2014) 409–418
doi:10.3993/jfbi09201410

A Fast Rigid Registration Algorithm for Medical Images

Yuncong Feng [a,b], Xiongfei Li [a,b,*], Xiaoli Zhang [a,b], Tienan Ding [a,b]

[a] *Key Laboratory of Symbolic Computation and Knowledge Engineering of Ministry of Education Changchun 130012, China*

[b] *Department of Computer Science and Technology, Changchun 130012, China*

Received 24 July 2013; accepted (in revised version) 13 June 2014; available online 23 September 2014

Abstract

Image registration is a vital research branch in medical image processing and analysis. In this paper, we proposed a new framework for rigid medical image registration. It can also be regarded as a pre-processing of non-rigid image registration algorithms. The interest of the algorithm lies in its simplicity and high efficiency. In the registration algorithm, we firstly segmented the reference image and float image into two parts: tissue parts and background parts. Then the centers of the two images were located through performing distance transform on the two segmented tissue images. Finally, we detected the longest radius of the two tissue regions, by which we determined the rotating angle. We tested the registration algorithm on dozens of medical images, and the experimental results show us that the algorithm is competent for medical image registration.

Keywords: Image Registration; Medical Image; Image Segment; Distance Transformation

1 Introduction

Image has become an important tool for information transfer and storage, and image processing techniques such as image registration, image fusion and image defect detection [1] are widely used to enhance the visual effect of the image and improve the image quality, and process some specific information contained in the image. As the foundation and key technology of modern medical image processing and analysis, medical image registration has crucial value on clinical application. It can be applied not only for the diagnosis of disease traits, but also in guiding the treatment process through tracking lesion sites, and evaluating the therapeutic effect. As far back as 1992, the main theories of image registration and image registration applications in various fields have been summarized by Lisa Gottesfeld Brown at the University of Cambridge in literature [2]. Currently, medical image registration technology has been widely used for image

*Corresponding author.
Email address: lxf@jlu.edu.cn (Xiongfei Li).

1940–8676 / Copyright © 2014 Binary Information Press & Textile Bioengineering and Informatics Society
September 2014

information fusion, three-dimensional image reconstruction, and image guided surgery to locate the spatial position relationships between images [3].

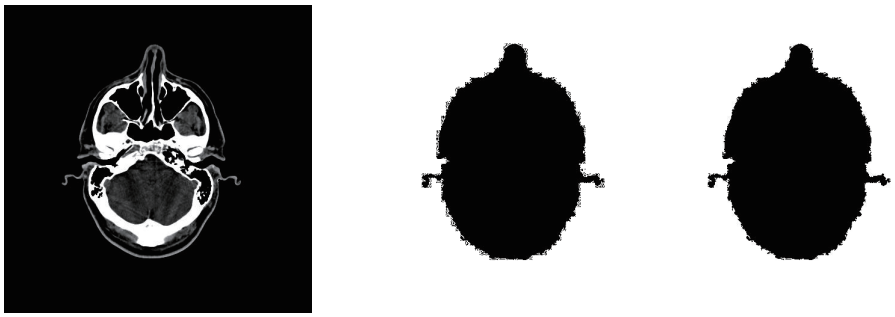
Actually, medical image registration is to seek one or a series of space transformations for one medical image using computer technology, and then, to make the corresponding points in this image achieve the same spatial position with another image. When all the anatomical points are matched, or at least the points with diagnostic significance and surgery points of interest are completed, image registration can be achieved. The main image registration techniques widely used nowadays are geometrical feature-based method [4] and pixel intensity-based method [5, 6]. The former has the characteristics of less calculation and high velocity, but its registration accuracy depends on feature extraction. The features can be marks, contours, planes, etc., or the combination between them. Brian C. Chalermwat et al. [7] presented a two-phase sequential and coarse-grained parallel image registration algorithm using genetic algorithm (GA) as optimization mechanism. Wang proposed to use Artificial Bee Colony to register images [8]. The latter, pixel intensity-based method, which is attracting most attention at present, takes advantage of the image data directly without pretreatment, thus, it avoids the error caused by feature extraction. For this reason, it is robust and relatively accurate. The method based on mutual information has high accuracy, and according to recent studies it is insensitive to incomplete image and noise [9]. Josien PW Pluim analyzed two interpolation methods in [10] linear interpolation and partial volume interpolationwhich are frequently used in mutual information-based image registration. Shun'ichi Kaneko presented a selective correlation coefficient method, which is available for image registration of bad light conditions and the curve is not completely closed [11]. Many medical image registration methods have been developed over decades, different angles with different classifications. Maintz et al. classified these methods from eight different angles, which is accepted by most scholars (for details see reference [12]). According to the nature of spatial transformation, image registration can be divided into rigid and non-rigid registration [13]. The latter includes affine, projection and nonlinear transformation. Projection transformation is mainly used for 2D/3D image registration, while affine and nonlinear transformation are mainly used for soft tissue image registration, especially the parts easily deformed or displaced, such as the abdomen and lungs. The rigid registration, basis of other registration transformation, includes only translation and rotating transformation. At present, rigid registration has been more matured, especially for brain images. Wein et al. developed a new method that is applied in surgical navigation. Using rigid and affine transformation model, the method achieved automatic registration between ultrasound scan images and CT images in corresponding layers after three-dimensional reconstruction [14]. However, the automatic performance and registration speed of rigid registration for medical images still needs to be solved urgently. We note that nearly all the existing registration algorithms contain at least interaction, which makes them register images in a real time. Therefore, there has been considerable interest in finding new methods to achieve rapid medical images rigid registration.

In our study, we put forward a fast algorithm for rigid registration. The interest of the algorithm lies in its simplicity and high efficiency. In the registration algorithm, we firstly segment the reference image and float image into two parts: tissue parts and background parts. Then the centres of the two images are located though performing distance transformation on the two segmented tissue images. Finally, we detect the longest radius of the two tissue regions, by which we determine the rotating angle. We test the registration algorithm on dozens of medical images, and the experimental results show us that the algorithm is competent for medical image registration.

The rest of this paper is organized as follows. Section 2 gives the process of medical image segmentation. In Section 3, we detail the procedure of our proposed registration method; Section 4 shows the performance of this new method experimentally; the main conclusions are summarized in Section 5.

2 Pre-processing

In medical image registration only the tissue parts are processed and the background parts are neglected which may be filled with the same gray-scale or the same colour, it is valuable to segment the original images into two parts: tissue parts and background parts before running registration algorithms. Fig. 1 shows us a CT of a brain. We notice that the background part is filled with black colour, while the tissue part is more complex relatively, it contains white colour such as bones, skin, and contains black regions as well. Based on the characteristic of the medical image, we adopt a region-growing-based image segmentation algorithm, which we name it as Bi-directional Region-Growing-based (BRG-based) image segmentation.



(a) (b) (c)

Fig. 1: Medical image segmentation

Let I denote the image to be segmented, the steps of BRG-based image segmentation are as follows:

Step 1: Select the seed which is located at the pixel (1, 1) and set the threshold $\boldsymbol{T}$.

Step 2: Check the neighbouring pixels and add them to the region (they are labelled by "0"), if they are similar to the seed. If the difference between a neighbouring pixel and the centre pixel is smaller than $\boldsymbol{T}$, we deem that they are similar.

Step 3: Repeat Step 2 for each of the newly added pixels.

Step 4: Label other pixels by "1".

Step 5: Select seed which is located at centre of regions labelled by "1".

Step 6: Check the neighbouring pixels and add them to the region (they are labelled by "1"), if they are the same to the seed.

Step 7: Repeat Step 6 for each of the newly added pixels; stop if no more pixels can be added.

Step 8: Label other pixels by "0".

Fig. 2 shows us the flowchart of regional growing algorithm. In effect, BRG-based image segmentation involves two regional growing steps. The two regional growing algorithms are the same except the initial seed selections and the threshold T settings.

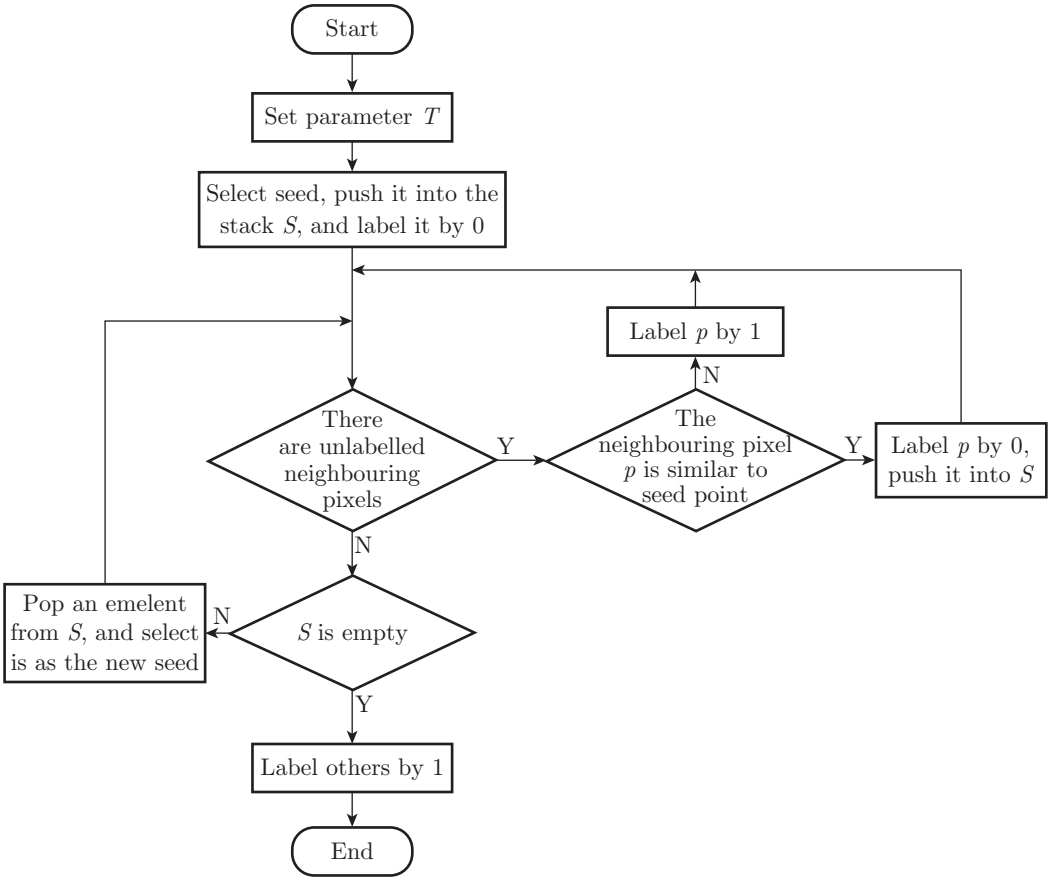


Fig. 2: The flowchart of regional growing algorithm

In Fig. 1 (b) is obtained by running the traditional region-growing-based algorithm. We noticed that there are many isolated small regions; the reason why these regions are generated is because the edge region is complex. In order to connect tissue part, the segmentation algorithm is run again with the seed at the centre of tissue part. The centre can be located though distance transformation (described in later subsection) or other methods. Therefore, we adopt the BRG-based image segmentation here. The subfigure 1-(c) is the result of the refined segmentation algorithms. The results show that it can tackle the problem that may be brought by traditional region-growing-based algorithms.

3 Proposed Algorithm

3.1 Distance Transform

The distance transform, as an operator normally only applies to binary images, it is a useful tool in the field of image analysis. It is adopted in our medical image registration algorithm to find the centers of tissue parts, and consequently determine the coefficients of shifting. In 2D Euclidean space, the distance transform is defined as

Definition 1: Let $A = \{p|l(p) = 1,\ p \in \mathrm{R}^2\}$ and $\bar{A} = \{q|l(q) = 0,\ q \in \mathrm{R}^2\}$, for any $p \in A$, its transform coefficient is $DT(p) = \min\{d(p, q)|q \in \bar{A}\}$.

In Definition, A denotes the pixel set belonging to the foreground, and $\bar{A}$ denotes the pixel set belonging to background. From the Definition 1, we note that the distance transform is to find the shortest distance of foreground pixels from background. Therefore, if a pixel obtains a smaller distance transform coefficient than another, the former one is step closer to the background regions; and vice versa. Based on the property of the Distance Transform, the centre of tissue parts of the medical images can be located, and consequently the shifting coefficients can be deduced.

Fig. 3 shows us an example of distance transformation. (a) is a binary image in which "0" means background, and "1" does objects. (b) shows the distance transforms coefficients of (a). In (b), the digit is the nearest distance of the corresponding pixels from the background regions.

0	0	0	0	0	0	0	0
0	1	1	1	1	1	1	0
0	1	1	1	1	1	1	0
0	1	1	1	1	1	1	0
0	1	1	1	1	1	1	0
0	1	1	1	1	1	1	0
0	1	1	1	1	1	1	0
0	0	0	0	0	0	0	0

(a)

0	0	0	0	0	0	0	0
0	1	1	1	1	1	1	0
0	1	2	2	2	2	1	0
0	1	2	3	3	2	1	0
0	1	2	3	3	2	1	0
0	1	2	2	2	2	1	0
0	1	1	1	1	1	1	0
0	0	0	0	0	0	0	0

(b)

Fig. 3: An example of distance transform: (a) A binary image; (b) The distance transform coefficients

After obtaining distance transform coefficients of reference image and float image, which are denoted by DT_R and DT_F, we can locate the centre of the tissue parts in the two images, the indexes of the centres in the two images are

$$c(R) = \arg\max DT_R(p) \tag{1}$$

and

$$c(F) = \arg\max DT_F(p) \tag{2}$$

And the shifting coefficient sc is defined as

$$sc = c(F) - c(R) \tag{3}$$

The procedure of shifting can be represented as

$$F_1(p + sc) = F(p) \tag{4}$$

After the shifting, the centre of float image is aligned to the one of the reference image.

3.2 Edge Detection

In this subsection, we aim at determining the angle of rotation of the float image. We note that nearly all the brain images are similar to elliptical shape, which give us a new insight into the determination of rotating angle: we can rotate the float image by making the longest radius of

the two brain images coincide with each other. The procedure of find rotation angles needs no iteration, so it is bound to be superior to other algorithms in efficiency.

The key issue here may be how to find out the longest radius. Here, we firstly, detect the edges of the two images based on the segmentation results, and then, calculate the Euclidean distance between edge pixels and center pixels.

Let B_R and B_F denote the segmentation results of reference image R and float image F. The edge pixels at least contains a different neighbouring pixel, while inside pixels are surrounded by peers which are labelled by the same label with it. So, the edge pixels of reference image R can be find by

$$E_R = \bigoplus_{i=1}^{8} D_{R,i} = D_{R,1} \oplus D_{R,2} \oplus D_{R,3} \oplus D_{R,4} \oplus D_{R,5} \oplus D_{R,6} \oplus D_{R,7} \oplus D_{R,8} \tag{5}$$

where, $D_{R,i} = |B_R - B_i|$. B_i is a matrix obtained by shifting B_R along with the angle of $i\pi/4$ with the step of 1 pixel. Using Eq. (5), we can also get the edge pixels of float image F, which is denoted by E_F.

Based on the E_R and E_F, we can get the edge pixels that are farthest from the centers in the reference image R and float image F. We denote the two pixels as $r(R)$ and $r(F)$. The rotation angle θ is defined as:

$$\theta = \arccos \frac{|(f(R) - r(R)) \cdot (f(F) - r(F))|}{|f(R) - r(R)| \cdot |f(F) - r(F)|} \tag{6}$$

Here, F_1 can be rotated with the angle $= \theta$, and the final image is denoted as F_2. Until now, two important coefficients are obtained: shifting coefficient sc and rotating coefficient θ. In the experimental parts, performance of the newly-proposed registration algorithm is tested by comparing the two coefficients with their true values.

4 Experimental Results

4.1 Experimental Settings

In this section, the newly proposed image registration algorithm is tested on dozens of image pairs, the original images come from the website (http://www.insight-journal.org/rire/). The website provides a variety of CT, MRI, PET images of brains. The parameter settings in the registration algorithm are as follows: the threshold $\boldsymbol{T}$ in BRG-based image segmentation algorithm (in Section 2) equals to 51(=0.2*255), The setting on dozens of medical images are tested, and the experimental results shows that the segmentation algorithm can successfully separate the tissue parts from the background parts, and consequently justify the rationality of $\boldsymbol{T}$'s setting. Another issue that needs to be considered is which type of distance should be adopted in the distance transformation (in subsection 3.1). There are generally four alternatives: "chessboard", "euclidean", "cityblock" and "quasi-euclidean". We note that the distance should be robust to rotation, so we choose "euclidean" distance in the implementation of our algorithms.

4.2 Single-modal Medical Image Registration

Clinically, Doctors may need to compare the medical images of patients captured before and after surgery to evaluate the effectiveness of surgery. The images captured by the same type of scanner, but the position of tissue parts in the images maybe different. In this case, these images needs to be registered for alignment. In this section, the registration algorithm is tested on single-modal medical image registration.

The test data is shown in Fig. 4 and Fig. 5. In each figure, (a) is reference image, (b) is the float image. The registered images of the float image are displayed in (c)-(f) by four algorithms: the proposed registration algorithm, the algorithm in [3], [15] and [16]. The float image is obtained by rotating the reference image 30 degrees, shifting down 70 pixels and shifting right 30 pixels.

The error of predicted values of sc and θ in Fig. 4 and Fig. 5 are shown in Table 1. A lower error means a better performance of the algorithm in the corresponding aspect.

Table 1: Predicted values of sc and θ

test image	error of sc				error of θ			
	(c)	(d)	(e)	(f)	(c)	(d)	(e)	(f)
Fig. 4	(4, 7)	(8, 8)	(7, 6)	(7, 10)	3.73	5.52	3.80	3.77
Fig. 5	(5, 3)	(6, 7)	(3, 6)	(8, 11)	5.79	6.68	8.21	4.21

From Table 1, we note that the predicted value obtained by the proposed algorithm is closer to the true value comparing to other registration algorithm, and it shows that the registration

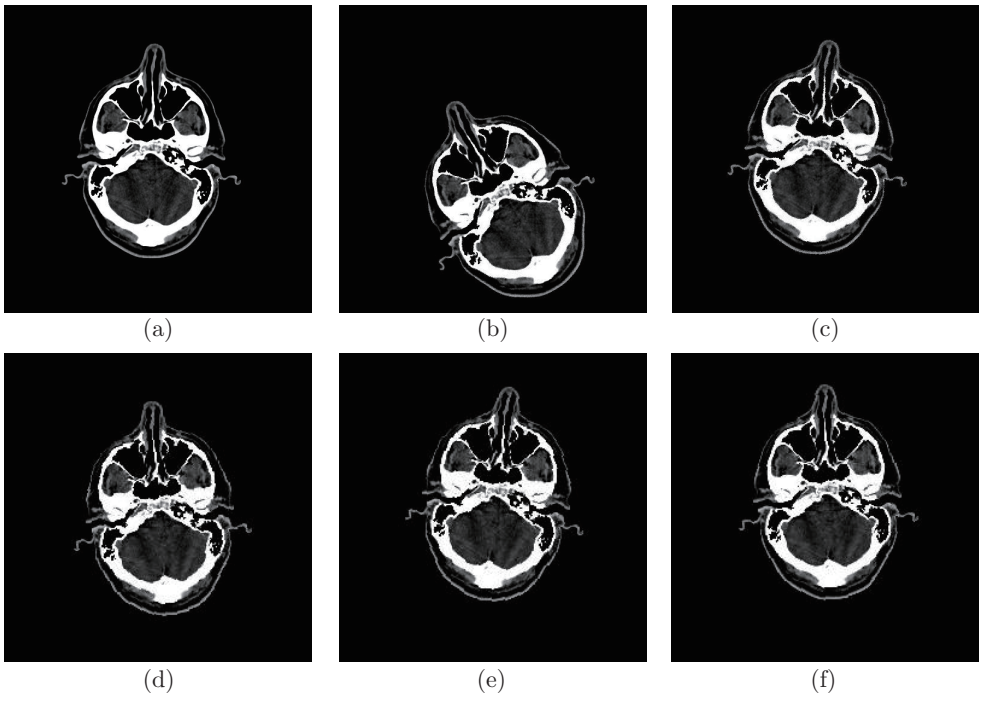
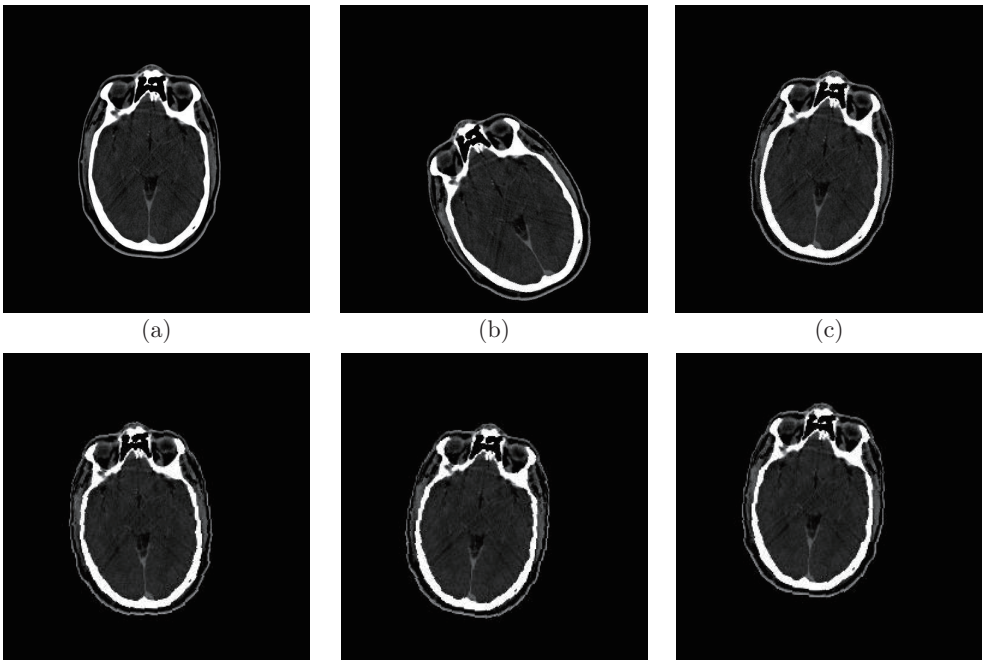


Fig. 4: Single-modal medical image registration (Group ID = #1): (a) Reference image; (b) Float image; (c) Our registered image; (d) Registered image by [3]; (e) Registered image by [15]; (f) Registered image by [16]

algorithm performs well.

4.3 Multiple-modal Medical Image Registration

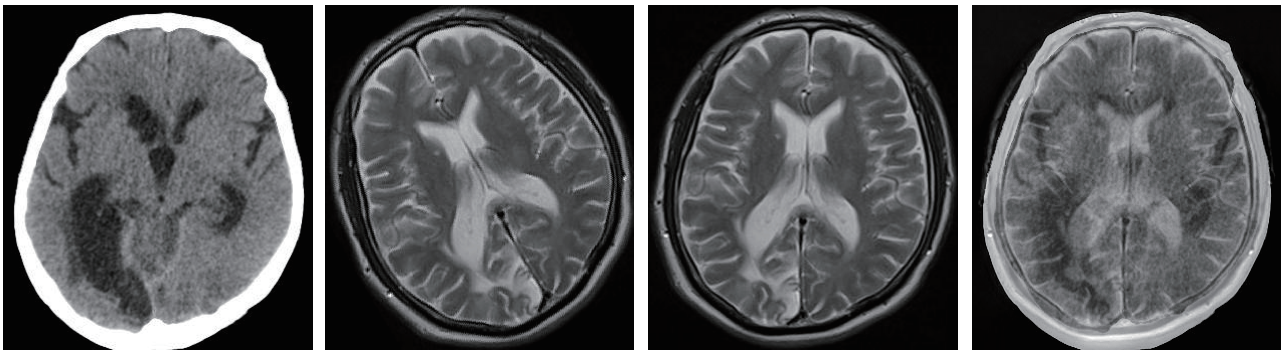
In modern medical imaging field, there is a variety of image type. They include Computer Tomography (CT), Magnetic Resonance Imaging (MRI), Positron Emission Computed Tomography (PET), Cerebral Blood Flow (CBF) and so on. They are captured by different scanners which are quite different from each other in the mechanism of imaging. All of them have their merits and demerits. For example, CT can explicitly show the bone, but can hardly show soft tissue parts. MRI, in contrast, can capture the soft tissue parts and fail in reflecting the bone. So, a lot of efforts have been made to combine CT and MRI images in a bid to achieve a more informative



(a) (b) (c)

(d) (e) (f)

Fig. 5: Single-modal medical image registration: (Group ID = #2): (a) Reference image; (b) Float image; (c) Our registered image; (d) Registered image by [3]; (e) Registered image by [15]; (f) Registered image by [16]



(a) CT image (b) MRI (c) Registered image (d) Fused image of (a) and (c)

Fig. 6: Multiple-modal medical image registration

image. Before combination, registration is needed to align these images.

In this subsection, we test our algorithm on multiple-modal medical image registration. The experimental images are shown in Fig. 6. Fig. 6 (a) is a CT image, Fig. 6 (b) is the MRI image. We can notice that the two type of images are quite different in structure. Fig. 6 (c) is the registered image of MRI by running our registration algorithm.

In most cases, image registration plays the role of pre-processing of fusion, so the CT image is fused with the registered MRI image, and the fusion result is shown in Fig. 6 (d). The fused image preserves the salient information of CT image and MRI images, and it also shows that the registration algorithm performs well.

5 Conclusions

In this paper, the problem of rigid medical image registration was investigated. The key advantage of the newly proposed registration algorithm was its simplicity and high efficiency. In the proposed algorithm, we firstly segmented the reference image and float image into two parts: tissue parts and background parts. Then the centers of the two images were located though performing distance transform on the two segmented tissue images. Finally, the longest radii of the two tissue regions are detected, and we determined the rotating angle with the assistance of the radii.

The registration algorithm was tested on dozens of medical images and experimental results to justify the superiority of the registration algorithm. However, the proposed algorithm just holds for brain image registration. So how to make it work when processing other types of medical images should be included in the future works.

Acknowledgements

The authors would like to express our gratitude to the editors and anonymous reviewers for their comments and suggestions. The work is supported by Technology Development Plan of Jilin Province with the contract number 20090468, 20100508, 201105017.

References

[1] Li PF, Yang J, Jing JF, Li JN. The high-speed fabric defect detection algorithm based on the image layered model. Journal of Fiber Bioengineering & Informatics 2013; 6(2): 161-173.

[2] Brown LG. A survey of image registration techniques. ACM Computing Surveys 1992; 24(4): P325-376.

[3] Chen HM, Varshney PK. Mutual information-based CT-MR brain image registration using generalized partial volume joint histogram estimation. IEEE Transactions on Medical Imaging 2003; 22(9): 1111-1119.

[4] Loeckx D, Slagmolen P, Maes F, Vandermeulen D, Suetens P. Nonrigid image registration using conditional mutual information. IEEE Transactions on Medical Imaging 2010; 29(1): 725-737.

[5] Kim J, Fessler JA. Intensity-based image registration using robust correlation coefficients. IEEE Transactions on Medical Imaging 2004; 23(11): 1430-1444.

[6] Hsu LY, Loew MH. Fully automatic 3D feature-based registration of multi-modality medical images. Image and Vision Computing 2001; 19 (1): 75-85.

[7] Chalermwat P, El-Ghazawi T, LeMoigne J. 2-phase GA-based image registration on parallel clusters. Future Generation Computer Systems 2001; 17: 467-476.

[8] Wang SH. Artificial bee colony used for rigid image registration. International Journal of Research and Reviews in Soft and Intelligent Computing 2011; 1: 33-36.

[9] Ding L, Goshtasby A, Satter M. Volume image registration by template matching. Image and Vision Computing 2001; 19(12): 821-832.

[10] Studholme C, Hill DLG, Hawkes DJ. Automated 3-D registration of MR and CT images of the head. Medical Image Analysis 1996; 1(2): 163-175.

[11] Pluim JPW, Maintz JBA, Viergever MA. Interpolation artifacts in mutual information-based image registration. Computer Vision and Image Understanding 2000; 77(22): 211-232.

[12] Kaneko S, Satoh Y, Igarashi S. Using selective correlation coefficient for robust image registration. Pattern Recognition 2003; 36(5): 1165-1173.

[13] Maint JBA, Viergever MA. A survey of medical image registration. Medical Image Analysis 1998; 2(l): l-36.

[14] Lee H, Lee JR. Feature-based registration using a gaussian weighted distance map and brain feature points for brain PET/CT image. Computers in Biology and Medicine 2008; 9(38): 945-961.

[15] Wein W, Brunke S, Khanmene A. Automatic CT-ultrasound registration for diagnostic imaging and image-guided intervention. Medical Image Analysis 2008; 12: 577-585.

[16] Martin S, Morison G, Nailon W, Durrani T. Fast and accurate image registration using Tsallis entropy and simultaneous perturbation stochastic approximation. Electron. Lett. 2004; 40(10): 595-597.